

1 **Optimal ENSO pattern that enhances large-scale atmospheric processes**
2 **conducive to tornado outbreaks in the U.S.**

3
4
5 Sang-Ki Lee^{1,2}, Robert Atlas², David Enfield^{1,2}, Hailong Liu^{1,2} and Chunzai Wang²

6 ¹Cooperative Institute for Marine and Atmospheric Studies, University of Miami, Miami,
7 Florida, USA

8 ²Atlantic Oceanographic and Meteorological Laboratory, NOAA, Miami Florida, USA
9 USA

10
11
12
13
14
15
16 October 2011

17
18
19
20
21
22 Corresponding author address: Dr. Sang-Ki Lee, NOAA/AOML, 4301 Rickenbacker Causeway,
23 Miami, FL 33149, USA. E-mail: Sang-Ki.Lee@noaa.gov.

1 **Abstract**

2 The record-breaking U.S. tornado outbreaks in the spring of 2011 prompt the need to identify
3 long-term climate signals that could potentially provide seasonal predictability for intense U.S.
4 tornado outbreaks. Here we show that a positive phase of Trans-Niño, characterized by cooling
5 in the central tropical Pacific and warming in the eastern tropical Pacific, may be one such
6 climate signal. The warming in the eastern tropical Pacific increases convection locally, but also
7 contributes to suppressing convection in the central tropical Pacific. This in turn works
8 constructively with cooling in the central tropical Pacific to force a persistent teleconnection
9 pattern that brings more cold and dry upper-level air from the high-latitudes and more warm and
10 moist lower-level air from the Gulf of Mexico converging into the U.S. east of the Rocky
11 Mountains, and also increases the lower-level vertical wind shear therein, thus providing large-
12 scale atmospheric conditions conducive to major tornado outbreaks over the U.S.

13
14
15
16
17
18
19
20
21
22
23

1 In April and May of 2011, a record breaking 1,061 tornadoes and 539 tornado-related
2 fatalities were confirmed in the U.S., making 2011 one of the deadliest tornado years in U.S.
3 history [<http://www.spc.noaa.gov/climo/torn/fataltorn.html>]. Questions were raised almost
4 immediately as to whether the series of extreme tornado outbreaks in 2011 could be linked to
5 long-term climate variability. The severe weather database (SWD) from the National Oceanic
6 and Atmospheric Administration indicates that the number of total U.S. tornadoes (i.e., from F0
7 to F5 in the Fujita scale) during the most active tornado months of April and May (AM) has been
8 steadily increasing since 1950 (Supplementary Fig. S1). However, due to numerous known
9 deficiencies in the SWD, including improvements in tornado detection technology, increased
10 eyewitness reports due to population increase, and changes in damage survey procedures over
11 time, one must be cautious in attributing this secular increase in the number of U.S. tornadoes to
12 a specific long-term climate signal^{1,2}.

13 In the U.S. east of the Rocky Mountains, cold and dry upper-level air from the high latitudes
14 often converges with warm and moist lower-level air coming from the Gulf of Mexico (GoM).
15 Due to this so-called large-scale differential advection (i.e., any vertical variation of the
16 horizontal advection of heat and moisture that decreases the vertical stability of the air column³),
17 conditionally unstable atmosphere with high convective available potential energy is formed.
18 The lower-level vertical wind shear associated with the upper-level westerly and lower-level
19 southeasterly winds (i.e., wind speed increasing and wind direction changing with height)
20 provides the spinning effect required to form a horizontal vortex tube. The axis of this horizontal
21 vortex tube can be tilted to the vertical by updrafts and downdrafts to form an intense rotating
22 thunderstorm known as a supercell, which is the storm type most apt to spawn intense
23 tornadoes^{4,5}. Consistently, both the moisture transport from the GoM to the U.S. and the lower-

1 level vertical wind shear in the central and eastern U.S. are positively correlated with U.S.
2 tornado activity in AM (Supplementary Table S1).

3 The Pacific - North American (PNA) pattern in boreal winter and spring is linked to the
4 large-scale differential advection and the lower-level vertical wind shear in the central and
5 eastern U.S.⁶⁻⁸. During a negative phase of the PNA, an anomalous cyclone is formed over North
6 America that bring more cold and dry upper-level air from the high latitudes to the U.S., and an
7 anomalous anticyclone is formed over the southeastern seaboard that increases the southwesterly
8 wind from the GoM to the U.S., thus enhancing the Gulf-to-U.S. moisture transport.
9 Additionally, the lower-level vertical wind shear is increased over the U.S. during a negative
10 phase of the PNA due to the increased upper-level westerly and lower-level southeasterly.
11 Although the PNA is a naturally occurring atmospheric phenomenon driven by intrinsic
12 variability of the atmosphere, a La Niña in the tropical Pacific can project onto a negative phase
13 PNA pattern^{9,10}. In addition, since the Gulf-to-U.S. moisture transport can be enhanced with a
14 warmer GoM, the sea surface temperature (SST) anomaly in the GoM can also affect U.S.
15 tornado activity. During the decay phase of La Niña in spring, the GoM is typically warmer than
16 usual¹¹. Therefore, the Gulf-to-U.S. moisture transport could be increased during the decay phase
17 of La Niña in spring due to the increased SSTs in the GoM and the strengthening of the
18 southwesterly wind from the GoM to the U.S. Nevertheless, none of these (i.e., PNA, GoM SST,
19 and La Nina) are highly correlated with U.S. tornado activity in AM (Supplementary Table S1).
20 Consistently, a recent study reported that the connectivity between the El Niño-Southern
21 Oscillation (ENSO) and U.S. tornado activity is quite weak¹². Currently, seasonal forecast skill
22 for intense U.S. tornado outbreaks, such as occurred in 2011, has not been demonstrated.

23

1 **Observed relationship between Trans-Niño and U.S. tornado activity**

2 Among the long-term climate patterns considered here (Supplementary Table S1), only the
3 Trans-Niño (TNI) is significantly correlated with U.S. tornado activity in AM. The TNI, which is
4 defined as the difference in normalized SST anomalies between the Niño-1+2 ($10^{\circ}\text{S} - 0^{\circ}$; $90^{\circ}\text{W} -$
5 80°W) and Niño-4 ($5^{\circ}\text{N} - 5^{\circ}\text{S}$; $160^{\circ}\text{E} - 150^{\circ}\text{W}$) regions, represents the evolution of ENSO in the
6 months leading up to the event and the subsequent evolution with opposite sign after the event¹³.
7 Given that AM is typically characterized with the development or decay phase of ENSO events,
8 it is more likely that the tropical Pacific SST anomalies in AM are better represented by the TNI
9 index than the conventional ENSO indices such as Niño-3.4 ($5^{\circ}\text{N} - 5^{\circ}\text{S}$; $170^{\circ}\text{W} - 120^{\circ}\text{W}$) or
10 Niño-3 ($5^{\circ}\text{N} - 5^{\circ}\text{S}$; $150^{\circ}\text{W} - 90^{\circ}\text{W}$)¹³. Nevertheless, it is not clear why U.S. tornado activity in
11 AM is more strongly correlated with the TNI index than with other ENSO indices.

12 It is noted that the historical time series for the number of intense (from F3 to F5 in the
13 Fujita-Pearson scale) tornadoes is characterized by intense tornado outbreak years, such as 1974,
14 1965 and 1957, embedded amongst much weaker amplitude fluctuations (Supplementary Fig.
15 2a). Since the majority of tornado-related fatalities occur during those extreme outbreak years,
16 here we focus our attention to those extreme years and associated climate signals. Therefore, we
17 ranked the years from 1950 to 2010 (61 years in total) based on the number of intense U.S.
18 tornadoes in AM.

19 The top ten extreme tornado outbreak years are characterized by an anomalous upper-level
20 cyclone over North America that advects more cold and dry air to the U.S. (Fig. 1a), increased
21 Gulf-to-U.S. moisture transport (Fig. 1b) and increased lower-level vertical wind shear over the
22 central and eastern U.S. (Fig. 1c), whereas the bottom ten years are associated with an
23 anomalous upper-level anticyclone over North America (Fig. 1d), decreased Gulf-to-U.S.

1 moisture transport (Fig. 1e) and decreased lower-level vertical wind shear over the central and
2 eastern U.S. (Fig. 1f). Note that if the tornado ranking is redone based on the intense U.S
3 tornado-days in AM, 1998 in the top ten list is replaced by 1960, but other top nine years remain
4 in the top ten.

5 As in the top ten extreme tornado outbreak years, the top ten positive TNI years are also
6 characterized by an anomalous upper-level cyclone over North America (Fig. 2a), increased
7 Gulf-to-U.S. moisture transport (Fig. 2b) and increased lower-level vertical wind shear over the
8 central and eastern U.S. (Fig. 2c). Consistently, among the top ten extreme tornado outbreak
9 years, seven years including the top three are identified with a positive phase (i.e., within the
10 upper quartile) TNI index (i.e., normalized SST anomalies are larger in the Niño-1+2 than in
11 Niño-4 region) (Table 1). Five out of those seven years are characterized by a La Niña
12 transitioning to a different phase or persisting beyond AM (1957, 1965, 1974, 1999, and 2008)
13 and the other two with an El Niño transitioning to either a La Nina or neutral phase (1983 and
14 1998). In the composite SST anomalies for those five positive phase TNI years transitioning
15 from a La Niña, the central tropical Pacific (CP) and the eastern tropical Pacific (EP) are
16 characterized by cooling and warming, respectively (Fig 3a).

17 On the other hand, among the bottom ten years (Supplementary Table S3), only one year is
18 identified with a positive phase TNI, and the other nine years are with a neutral phase TNI (i.e.,
19 between the lower and upper quartiles), suggesting that a negative phase of the TNI neither
20 decreases nor increases the number of intense U.S. tornadoes in AM. Interestingly, four years
21 among the bottom ten years are identified with a La Niña transitioning to a different phase or
22 persisting beyond AM (1950, 1951, 1955 and 2001), and four are identified with an El Niño
23 transitioning to a different phase or persisting beyond AM (1958, 1987, 1988 and 1992). The

1 composite SST anomaly pattern for the four years of the bottom ten years with a La Niña
2 transitioning is that of a typical La Niña with the SST anomalies in the Niño-4 and Niño-1+2
3 being both strongly negative (i.e., neutral phase TNI) (Fig. 3b). Similarly, the composite SST
4 anomaly pattern for the four years in the bottom ten years with an El Niño transitioning is that of
5 a typical El Niño with the SST anomalies in the Niño-4 and Niño-1+2 being both strongly
6 positive (i.e., neutral phase TNI) (Fig. 3c).

7 In summary, observations seem to indicate that a positive phase of the TNI (i.e., normalized
8 SST anomalies are larger in the Niño-1+2 than in Niño-4 region) is linked to increased U.S.
9 tornado activity in AM, whereas either La Niñas and El Niños with a neutral phase TNI (i.e., the
10 SST anomalies in the Niño-1+2 region are as strong and the same sign as the SST anomalies in
11 the Niño-4) are not linked to increased U.S. tornado activity in AM.

12

13 **Simulated impact of TNI on tornadic environments**

14 To explore the potential link between the three tropical Pacific SST anomaly patterns identified
15 in the previous section (Fig. 3) and U.S. tornado activity in AM, a series of AGCM experiments
16 are performed. In EXP_TNI (Fig. 4), an anomalous upper-level cyclone is formed over North
17 America that brings more cold and dry air to the U.S., and both the Gulf-to-U.S. moisture
18 transport and the lower-level vertical wind shear over the central and eastern U.S. are increased,
19 all of which are large-scale atmospheric conditions conducive to intense tornado outbreaks over
20 the U.S.

21 In EXP_ELN (Supplementary Fig. S3), on the other hand, the Gulf-to-U.S. moisture
22 transport is neither increased nor decreased. The lower-level vertical wind shear is slightly
23 decreased over the central and eastern U.S. mainly due to a weak anomalous upper-level

1 anticyclone formed over North America. In EXP_LAN (Supplementary Fig. S3), a relatively
2 weak anomalous upper-level cyclone is formed, and thus the lower-level vertical wind shear is
3 slightly increased. However, the Gulf-to-U.S. moisture is not increased.

4 Therefore, these model results support the hypothesis that a positive phase of the TNI with
5 cooling in CP and warming in EP enhances the large-scale differential advection in the central
6 and eastern U.S. and increases the lower-level vertical wind shear therein, thus providing large-
7 scale atmospheric conditions conducive to intense tornado outbreaks over the U.S. However, the
8 model results do not show favorable large-scale atmospheric conditions in the central and eastern
9 U.S. under La Niña and El Niño conditions as long as the SST anomalies in EP are as strong and
10 the same sign as the SST anomalies in CP.

11

12 **CP- versus EP-forced teleconnection**

13 The model results strongly suggest that cooling in CP and warming in EP may have a
14 constructive influence on the teleconnection pattern that strengthens the large-scale differential
15 advection and lower-level vertical wind shear over the central and eastern U.S. To better
16 understand how the real atmosphere with moist diabatic processes responds to CP cooling and
17 EP warming, two sets of additional model experiments (EXP_CPC and EXP_EPW) are
18 performed (Supplementary Table S3).

19 In EXP_CPC (Fig. 5), the teleconnection pattern emanating from the tropical Pacific consists
20 of an anticyclone over the Aleutian Low in the North Pacific, a cyclone over North America, and
21 an anticyclone over the southeastern U.S. extending to meso-Americas, consistent with a
22 negative phase PNA-like pattern (Fig. 5a). As expected from the anomalous anticyclonic
23 circulation over the southeastern U.S. and meso-America, the Gulf-to-U.S. moisture transport is

1 increased in EXP_CPC (Fig. 5b). The lower-level vertical wind shear is increased over the
2 central and eastern U.S. due to the strengthening of the upper-level westerly and lower-level
3 southeasterly winds (Fig. 5c).

4 Surprisingly, the Rossby wave train forced by warming in EP (EXP_EPW) is very similar to
5 that in EXP_CPC (Fig. 5d). Consistently, both the Gulf-to-U.S. moisture transport and the lower-
6 level vertical wind shear over the central and eastern U.S. are also increased in EXP_EPW as in
7 EXP_CPC and EXP_TNI (Fig. 5e and f). A question arises as to why the teleconnection pattern
8 forced by warming in EP is virtually the same as that forced by cooling in CP. It appears that the
9 Rossby wave train in EXP_EPW is not directly forced from EP. In EXP_EPW, convection is
10 increased locally in EP, but it is decreased in CP as in EXP_CPC (Supplementary Fig. S4c). This
11 suggests that increased convection in EP associated with the increased local SSTs suppresses
12 convection in CP that in turn forces a negative phase PNA-like pattern. Therefore, these model
13 results confirm that cooling in CP and warming in EP do have constructive influence on the
14 teleconnection pattern that strengthens the large-scale differential advection and lower-level
15 vertical wind shear over the central and eastern U.S. The model results also suggest that cooling
16 in CP with neutral SST anomalies in EP or warming in EP with neutral SST anomalies in CP can
17 strengthen the large-scale differential advection and lower-level vertical wind shear over the
18 central and eastern U.S.

19 An apparently important question is why warming in EP does not directly excite a Rossby
20 wave train to the high-latitudes. As shown in earlier theoretical studies, the vertical background
21 wind shear is one of the two critical factors required for tropical heating to radiate barotropic
22 teleconnections to the high-latitudes¹⁴. In both observations and EXP_CLM, the background
23 vertical wind shear between 200 and 850 hPa in AM is largest in the central tropical North

1 Pacific and smallest in EP and the western tropical Pacific (WP), providing an explanation as to
2 why the Rossby wave train in EXP_EPW is not directly forced in EP (Supplementary Fig. S5).

3

4 **Implications for a seasonal outlook for extreme U.S. tornado outbreaks**

5 The conclusion so far is that a positive phase of the TNI, characterized by cooling in CP and
6 warming in EP, strengthens the large-scale differential advection and lower-level vertical wind
7 shear in the central and eastern U.S., and thus provides favorable large-scale atmospheric
8 conditions for major tornado outbreaks over the U.S. However, the TNI explains only up to 10%
9 of the total variance in the number of intense U.S. tornadoes in AM. This suggests that intrinsic
10 variability in the atmosphere may overwhelm the TNI-teleconnection pattern over North
11 America as discussed in earlier studies for El Niño-teleconnection patterns in the Pacific–North
12 American region¹⁵. In other words, the predictability of U.S. tornado activity, which can be
13 defined as a ratio of the climate signal (the TNI index in this case) relative to the climate noise, is
14 low.

15 Nevertheless, seven of the ten most extreme tornado outbreak years during 1950-2010
16 including the top three years are characterized by a strongly positive phase of the TNI (Table 1).
17 A practical implication of this result is that a seasonal outlook for extreme U.S. tornado
18 outbreaks may be achievable if a seasonal forecasting system has significant skill in predicating
19 the TNI and associated teleconnections to the U.S. Obviously, before we can achieve such a
20 goal, there remain many crucial scientific questions to be addressed to refine the predictive skill
21 provided by the TNI and to explore other long-term climate signals that can provide additional
22 predictability in seasonal and longer time scales.

23

1 **U.S. Tornado Outbreaks in 2011**

2 A positive phase of the TNI prevailed during AM of 2011 with cooling in CP and warming EP
3 (Supplementary Fig. S6). An important question is whether the series of extreme U.S. tornado
4 outbreaks during AM of 2011 can be attributed to this positive phase of the TNI. During AM of
5 2011, an anomalous upper-level cyclone was formed over the northern U.S. and southern Canada
6 (Supplementary Fig. S7a), the Gulf-to-US moisture was greatly increased (Supplementary Fig.
7 S7b), and the lower-level vertical wind shear was increased over the central U.S., all indicating
8 the coherent teleconnection response to a positive phase of the TNI.

9 A distinctive feature in the 2011 TNI event is warming in WP (Supplementary Fig. S6).
10 Further experiments (Supplementary Table S3) suggest that the warming in WP indirectly
11 suppresses convection in CP, and thus works constructively with the cooling in CP to force a
12 strong and persistent negative phase PNA-like pattern (Supplementary Fig. S9 and S10). Thus, it
13 is highly likely that the 2011 positive phase TNI event did contribute to the U.S. tornado
14 outbreak in AM of 2011 by enhancing the differential advection and lower-level vertical wind
15 shear in the central and eastern U.S.

16 One of the caveats in this study, as in any tornado related climate research, is an artificial
17 inhomogeneity in the tornado database. Eyewitness reports are important sources for tornado
18 count, which can be affected by population growth and migration. Additionally, tornado rating is
19 largely based on structural damage - wind speed relationship, which can change with time and
20 case-by-case because every particular tornado - structure interaction is different in detail. For
21 these and other reasons, the historical time series of the tornado database cannot be completely
22 objective or consistent over time¹⁶. In this study, only the intense U.S. tornadoes (F3 - F5) are
23 selected and used since intense and long-lived tornadoes are less likely to be affected by,

1 although not completely free from, such issues in the tornado database. An alternative approach
2 is to develop and use a proxy tornado database, which can be derived from tornadic
3 environmental conditions in atmospheric reanalysis products. Results from recent studies that
4 used such an approach were promising^{17,18}.

6 **Methods**

7 **U.S. Tornado index.** Since intense and long-lived tornadoes are much more likely to be detected
8 and reported even before a national network of Doppler radar was build in the 1990s, only the
9 intense U.S. tornadoes (i.e., from F3 to F5 in the Fujita-Pearson scale) in AM during 1950-2010
10 from the SWD are selected and used in this study. The number of intense U.S. tornadoes is used,
11 after detrending, as the primary diagnostic index (Supplementary Fig. S1b). Another tornado
12 metric used in this study is the intense U.S. tornado-days, which is obtained by counting the
13 number of days in which more than a threshold number of intense tornadoes occurred²
14 (Supplementary Fig. S1c and d). The threshold number selected in this case is three and above,
15 which roughly represents the upper 25% in the number of intense U.S. tornadoes in a given day
16 of AM during 1950-2010. In general, the tornado count index is sensitive to big tornado outbreak
17 days, such as April 3, 1974 during which 60 intense tornadoes occurred over the U.S. The
18 tornado-days index is on the other hand put little weight on big tornado days. Since these two
19 tornado indices are complementary to each other, it is beneficial to use both of these indices. The
20 two tornado indices are further detrended and used by using a simple least squares linear
21 regression.

22

1 **EXP_TNI, EXP_LAN, EXP_ELN and EXP_CLM.** To explore the potential link between the
2 three tropical Pacific SST anomaly patterns identified in the previous section (Fig. 3) and the
3 number of intense U.S. tornadoes in AM, a series of AGCM experiments are performed by using
4 version 3.1 of the NCAR community atmospheric model coupled to a slab mixed layer ocean
5 model (CAM3). The model is a global spectral model with a triangular spectral truncation of the
6 spherical harmonics at zonal wave number 42. It is vertically divided into 26 hybrid sigma-
7 pressure layers. Model experiments are performed by prescribing various composite evolutions
8 of SSTs in the tropical Pacific region (15°S–15°N; 120°E-coast of the Americas) while
9 predicting the SSTs outside the tropical Pacific using the slab ocean model. To prevent
10 discontinuity of SST around the edges of the forcing region, the model SSTs of three grid points
11 centered at the boundary are determined by combining the simulated and prescribed SSTs. Each
12 ensemble consists of ten model integrations that are initialized with slightly different conditions
13 to represent intrinsic atmospheric variability. The same methodology was previously used for
14 studying ENSO teleconnection to the tropical North Atlantic region¹⁹.

15 Four sets of ensemble runs are performed (Supplementary Table S3). In the first experiment
16 (EXP_CLM), the SSTs in the tropical Pacific region are prescribed with climatological SSTs. In
17 the second experiment (EXP_TNI), the composite SSTs of the positive phase TNI years
18 identified among the ten most active U.S. tornado years are prescribed in the tropical Pacific
19 region. Note that only the five positive TNI years transitioning from a La Niña (1957, 1965,
20 1974, 1999, and 2008) are considered here because the other two positive TNI years are
21 transitioning from an El Niño (1983 and 1998) and thus tend to cancel the tropical SST
22 anomalies of the other five. In the next two experiments, the SSTs in the tropical Pacific region
23 are prescribed with the composite SSTs of the four years in the bottom ten years with a La Niña

1 transitioning (1950, 1951, 1955 and 2001) for EXP_LAN, and the four years in the bottom ten
2 years with an El Niño transitioning (1958, 1987, 1988 and 1992) for EXP_ELN.

3
4 **EXP_CPC and EXP_EPW.** To further understand how the real atmosphere with moist diabatic
5 processes responds to CP cooling and EP warming, two sets of additional model experiments
6 (EXP_CPC and EXP_EPW) are performed (Supplementary Table S3). These two experiments
7 are basically identical to EXP_TNI except that the composite SSTs of the positive phase TNI
8 years are prescribed only in the western and central tropical Pacific region (15°S–15°N; 120°E -
9 110°W) for EXP_CPC and only in the eastern tropical Pacific region (15°S–15°N; 110°W-coast
10 of the Americas) for EXP_EPW.

11
12 **EXP_011 and EXP_WPW.** A set of model experiments (EXP_011) is performed by prescribing
13 the SSTs for 2010 - 2011 in the tropical Pacific region while predicting the SSTs outside the
14 tropical Pacific using the slab ocean model (Supplementary Table S3). EXP_WPW is identical to
15 EXP_011 except that the SSTs for 2010 – 2011 are prescribed only in the western tropical
16 Pacific region (15°S–15°N; 120°E - 180°). (Supplementary Table S3).

17
18 **Acknowledgments.** We would like to thank Herold Brooks, Charles Doswell, Brian Mapes and
19 Gregory Carbin for their thoughtful comments and suggestions, which led to a significant
20 improvement of the paper. This study was motivated and benefited from interactions with
21 scientists at NOAA ESRL, GFDL, CPC, NCDC and AOML. In particular, we wish to thank
22 Wayne Higgins, Tom Karl and Marty Hoerling for initiating and leading discussions that
23 motivated this study. This work was supported by grants from the National Oceanic and

1 Atmospheric Administration's Climate Program Office and by grants from the National Science
2 Foundation.

3

4 **References**

- 5 1. Brooks, H. E. & Doswell III, C. A. Some aspects of the international climatology of
6 tornadoes by damage classification. *Atmos. Res.* **56**, 191–201 (2001).
- 7 2. Verbout, S. M., Brooks, H. E., Leslie, L. M. & Schultz, D. M. Evolution of the U.S. tornado
8 database: 1954-2003. *Wea. Forecasting* **21**, 86-93 (2006).
- 9 3. Whitney Jr., L. F., & Miller, J. E. Destabilization by differential advection in the tornado
10 situation 8 June 1953. *Bull. Amer. Meteor. Soc.* **37**, 224–229 (1956).
- 11 4. Lemon, L. R., Doswell III, C. A. Severe thunderstorm evolution and mesocyclone structure
12 as related to tornadogenesis. *Mon. Wea. Rev.* **107**, 1184–1197 (1979).
- 13 5. Doswell III, C. A. & Bosart, L. F. Extratropical synoptic-scale processes and severe
14 convection. Severe Convection Storms. *Meteor. Monogr.* **28**, Amer. Meteor. Soc. 27-69
15 (2001).
- 16 6. Horel, J. D. & Wallace, J. M. Planetary-scale atmospheric phenomena associated with the
17 Southern Oscillation. *Mon. Wea. Rev.* **109**, 813–829 (1981).
- 18 7. Wallace, J. M. & Gutzler, D. S. Teleconnections in the geopotential height field during the
19 Northern Hemisphere winter. *Mon. Wea. Rev.* **109**, 784–804 (1981).
- 20 8. Barnston A. G. & Livezey R. E. Classification, seasonality, and persistence of low-frequency
21 atmospheric circulation patterns. *Mon. Weather Rev.* **115**: 1083–1126 (1987).
- 22 9. Lau, K.-M. & Lim, H. On the dynamics of equatorial forcing of climate teleconnections. *J.*
23 *Atmos. Sci.*, **41**, 161–176 (1984).

- 1 10. Straus, D. M. & Shukla, J. Does ENSO force the PNA?, *J. Clim.*, **15**, 2340–2358 (2002).
- 2 11. Alexander, M. & Scott, J. The influence of ENSO on air-sea interaction in the Atlantic.
- 3 *Geophys. Res. Lett.*, **29**, 1701, doi:10.1029/2001GL014347 (2002).
- 4 12. Cook, A. R. & Schaefer, J. T. The relation of El Niño–Southern Oscillation (ENSO) to
- 5 winter tornado outbreaks, *Mon. Wea. Rev.*, **136**, 3121–3137 (2008).
- 6 13. Trenberth, K. E. & Stepaniak, D. P. Indices of El Niño evolution, *J. Clim.*, **14**, 1697–1701
- 7 (2001).
- 8 14. Lee, S.-K., Wang, C. & Mapes, B. E. A simple atmospheric model of the local and
- 9 teleconnection responses to tropical heating anomalies. *J. Clim.*, **22**, 272-284 (2009).
- 10 15. Hoerling, M. P & Kumar, A. Why do North American climate anomalies differ from one El
- 11 Niño event to another?, *Geophys. Res. Lett.*, **24**, 1059-1062 (1997).
- 12 16. Doswell III, C. A., Brooks, H. E. & Dotzek, N. On the implementation of the Enhanced
- 13 Fujita Scale in the USA. *Atmos. Res.*, **93**, 554-563, doi:10.1016/j.atmosres.2008.11.003
- 14 (2009).
- 15 17. Brooks, H. E., Lee, J. W. & Cravenc, J. P. The spatial distribution of severe thunderstorm
- 16 and tornado environments from global reanalysis data, *Atmos. Res.*, **67-68**, 73-94 (2003).
- 17 18. Weaver, S. J., Baxter, S. & Kumar, A. Climatic role of North American low-level jets on
- 18 U.S. regional tornado activity. *J. Climate*, submitted (2011).
- 19 19. Lee, S.-K., Enfield D. B. & Wang, C., Why do some El Ninos have no impact on tropical
- 20 North Atlantic SST? *Geophys. Res. Lett.*, **35**, L16705, doi:10.1029/2008GL034734 (2008).

21

22

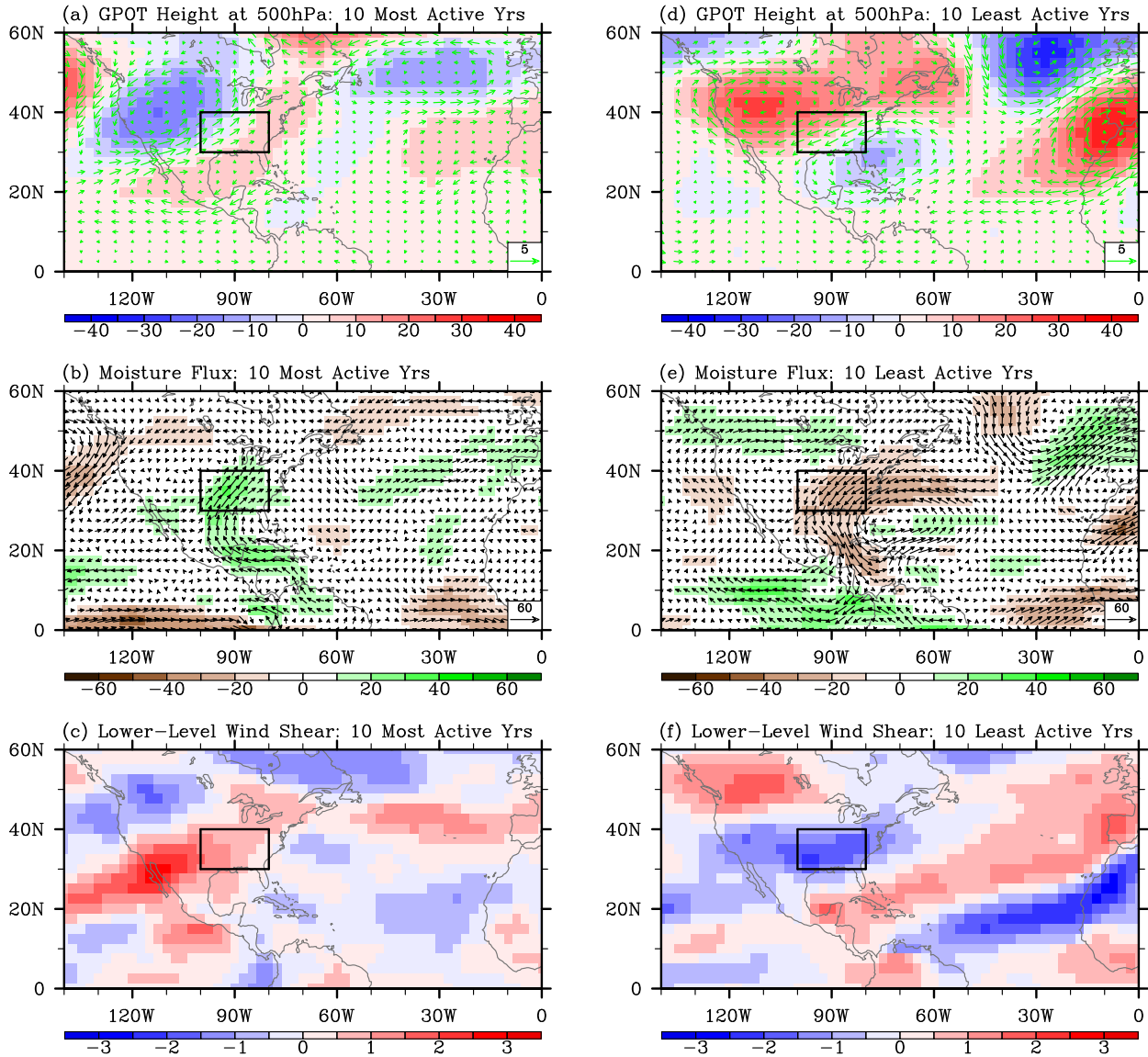
23

1 **Table 1.** The total of 61 years from 1950 to 2010 are ranked based on the detrended number of
 2 intense U.S. tornadoes in AM. The top ten extreme U.S. tornado outbreak years are listed with
 3 ENSO phase in spring and TNI index in AM for each year. Strongly positive (i.e., the upper
 4 quartile) and negative (i.e., the lower quartile) TNI index values are in bold and italic,
 5 respectively.

Ranking	Year	ENSO phase in spring	TNI index (detrended)
1	1974	La Niña persists	1.30 (1.48)
2	1965	La Niña transitions to El Niño	1.39 (1.54)
3	1957	La Niña transitions to El Niño	0.57 (0.69)
4	1982	El Niño develops	<i>-1.11 (-0.89)</i>
5	1973	El Niño transitions to La Niña	<i>-0.42 (-0.24)</i>
6	1999	La Niña persists	0.47 (0.75)
7	1983	El Niño decays	1.86 (2.08)
8	2003	El Niño decays	<i>-1.24 (-0.94)</i>
9	2008	La Niña decays	1.41 (1.73)
10	1998	El Niño transitions to La Niña	1.69 (1.97)

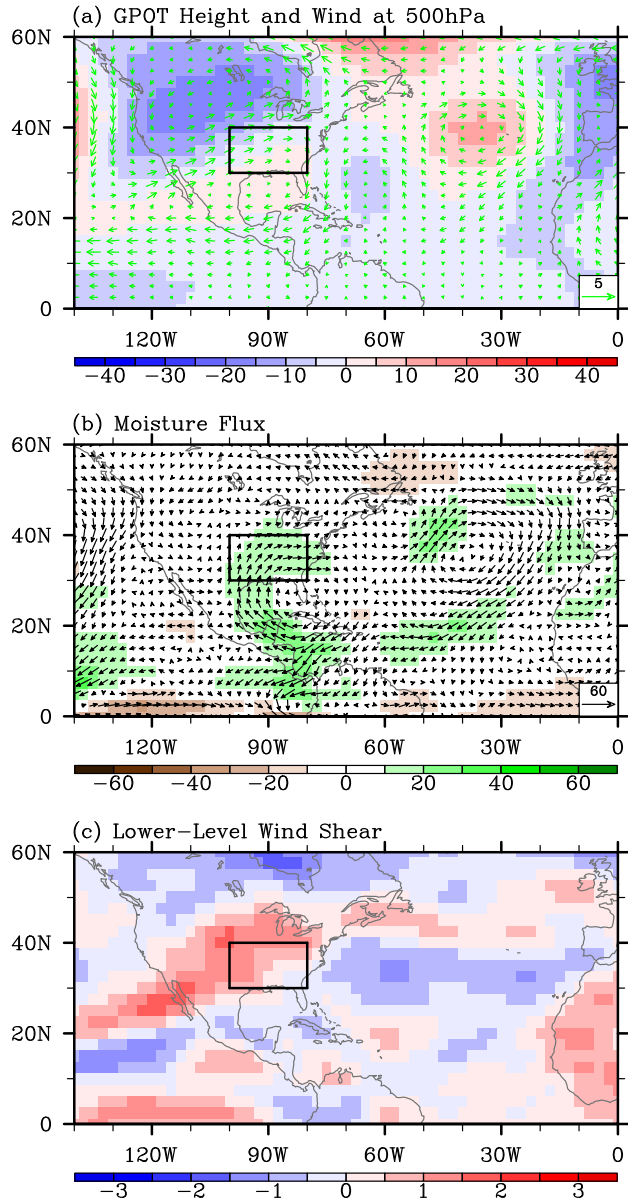
6

NCEP-NCAR Reanalysis: Key Atmospheric Conditions during Active and Inactive Years (APR-MAY)



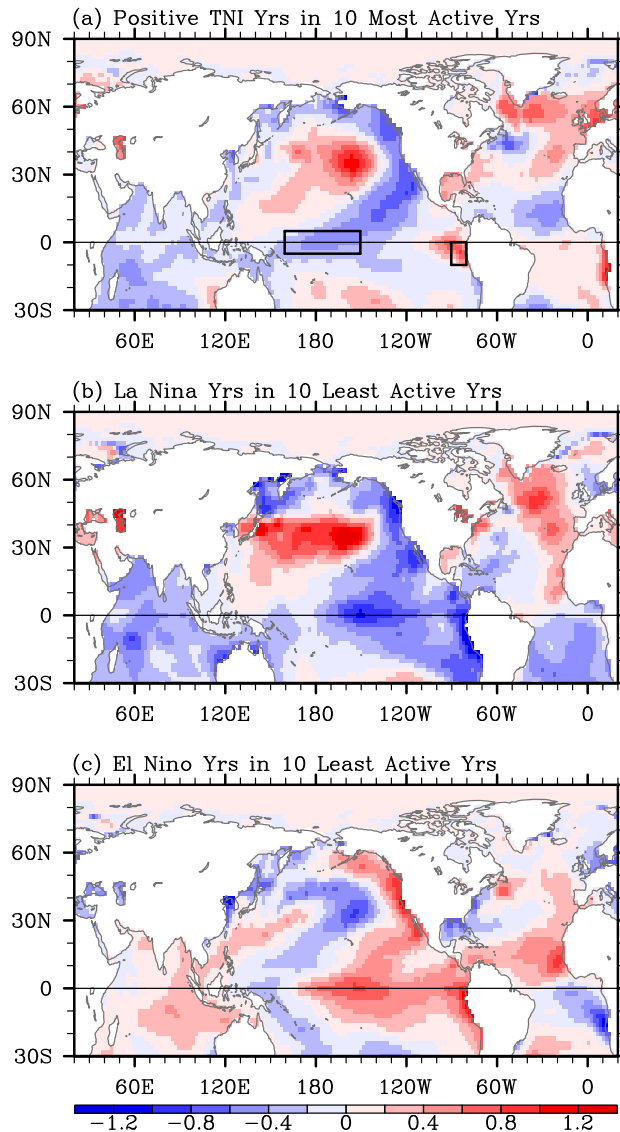
1
 2 **Figure 1.** Anomalous geopotential height and wind at 500 hPa, moisture transport and lower-
 3 level (500 hPa – 925 hPa) vertical wind shear for the ten most active U.S. tornado years (a, b and
 4 c) and the ten least active U.S. tornado years (d, e and f) in AM during 1950-2010 obtained from
 5 NCEP-NCAR reanalysis. The units are kg m⁻¹sec⁻¹ for moisture transport, m for geopotential
 6 height, and m s⁻¹ for wind and wind shear. The small box in (a) - (f) indicates the central and
 7 eastern U.S. region frequently affected by intense tornadoes.

NCEP-NCAR Reanalysis: Pos. TNI Years (APR-MAY)



1
2 **Figure 2.** Anomalous (a) geopotential height and wind at 500 hPa, (b) moisture transport and (c)
3 lower-level (500 hPa – 925 hPa) vertical wind shear for the top ten positive TNI years in AM
4 during 1950-2010 obtained from NCEP-NCAR reanalysis. The units are $\text{kg m}^{-1}\text{sec}^{-1}$ for moisture
5 transport, m for geopotential height, and m s^{-1} for wind and wind shear. The small box in (a) - (c)
6 indicates the central and eastern U.S. region frequently affected by intense tornadoes.

ERSST3: SST Anomalies (APR-MAY)

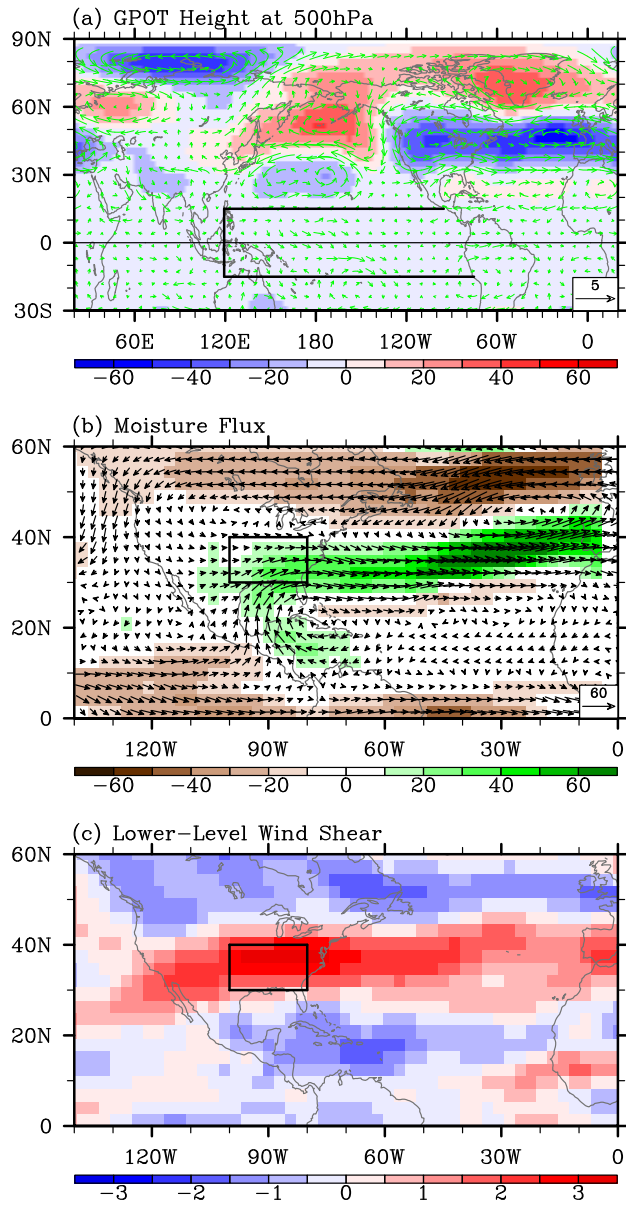


1

2 **Figure 3.** Composite SST anomalies in AM, obtained from ERSST3, for (a) the five positive
3 TNI years transitioning from a La Niña identified among the ten most active U.S. tornado years
4 in AM during 1950-2010, and for (b) the four years with a La Niña transitioning and (c) the four
5 years with an El Niño transitioning identified among the ten least active U.S. tornado years in
6 AM during 1950-2010. Thick black rectangles in (a) indicate the Niño-4 (5°N - 5°S; 160°E -
7 150°W) and Niño-1+2 (10S° - 0°; 90°W - 80°W) regions.

8

CAM3: EXP_TNI - EXP_CLM (APR-MAY)



1
2 **Figure 4.** Simulated anomalous (a) geopotential height and wind at 500 hPa, (b) moisture
3 transport and (c) lower-level (500 hPa – 925 hPa) vertical wind shear in AM obtained from
4 EXP_TNI – EXP_CLM. The units are $\text{kg m}^{-1} \text{sec}^{-1}$ for moisture transport, m for geopotential
5 height, and m s^{-1} for wind and wind shear. Thick black lines in (a) indicate the tropical Pacific
6 region where the model SSTs are prescribed. The small box in (b) and (c) indicates the central
7 and eastern U.S. region frequently affected by intense tornadoes.

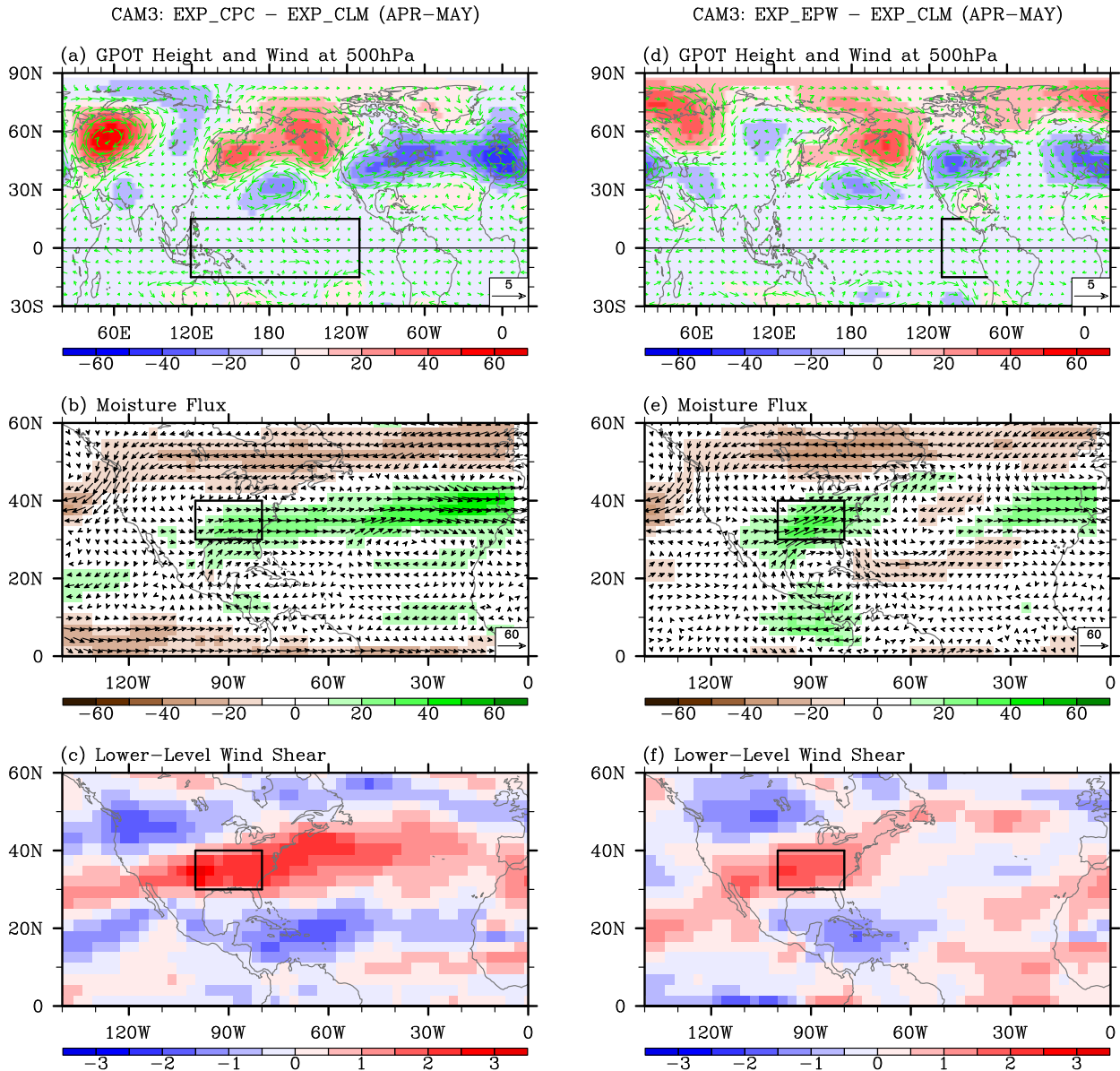


Figure 5. Simulated anomalous geopotential height and wind at 500 hPa, moisture transport, and lower-level (500 hPa – 925 hPa) vertical wind shear in AM obtained from EXP_CPC – EXP_CLM (a, b and c), and EXP_EPW – EXP_CLM (d, e and f). The units are $\text{kg m}^{-1} \text{sec}^{-1}$ for moisture transport, m for geopotential height, and m s^{-1} for wind and wind shear. Thick black lines in (a) and (d) indicate the regions where the model SSTs are prescribed. The small box in (b), (c), (e) and (f) indicates the central and eastern U.S. region frequently affected by intense tornadoes.

Table S1. Correlation coefficients of various long-term climate patterns in December-February (DJF), February-April (FMA), and April and May (AM) with the number of intense tornadoes in AM during 1950-2010. The values in parenthesis are those with the intense U.S. tornado-days in AM during 1950-2010. All indices including the tornado index are detrended using a simple least squares linear regression. The SWD, ERSST3, and NCEP-NCAR reanalysis are used to obtain the long-term climate indices used in this table. Correlation coefficients above the 95% significance are in bold^a.

Index	DJF	FMA	AM
Gulf-to-U.S. moisture transport	0.08 (0.05)	0.20 (0.14)	0.40 (0.36)
Lower-level vertical wind shear	0.06 (0.04)	0.15 (0.25)	0.34 (0.30)
GoM SST	0.15 (0.15)	0.21 (0.16)	0.20 (0.19)
Niño-4	-0.22 (-0.19)	-0.20 (-0.18)	-0.19 (-0.18)
Niño-3.4	-0.13 (-0.11)	-0.13 (-0.12)	-0.11 (-0.11)
Niño-1+2	0.02 (0.03)	0.11 (0.11)	0.15 (0.13)
TNI	0.28 (0.26)	0.29 (0.28)	0.33 (0.29)
PNA	-0.05 (-0.02)	-0.10 (-0.06)	-0.20 (-0.16)
PDO	-0.12 (-0.09)	-0.10 (-0.11)	-0.14 (-0.20)
NAO	-0.01 (-0.07)	-0.10 (-0.14)	-0.18 (-0.18)

^aThe Gulf-to-U.S. meridional moisture transport is obtained by averaging the vertically integrated moisture transport in the region of 25°N - 35°N and 100°W - 90°W. The lower-level (500 hPa – 925 hPa) vertical wind shear is averaged over the region of 30°N – 40°N and 100°W – 80°W. The North Atlantic Oscillation (NAO) index and the Pacific - North American (PNA) pattern are defined as the first and second leading modes of Rotated Empirical Orthogonal Function (REOF) analysis of monthly mean geopotential height at 500 hPa, respectively. The Pacific Decadal Oscillation (PDO) is the leading principal component of monthly SST anomalies in the North Pacific Ocean north of 20°N.

Table S2. The total of 61 years from 1950 to 2010 are ranked based on the detrended number of intense U.S. tornadoes in AM. The bottom ten years are listed with ENSO phase in spring and TNI index in AM for each year. Strongly positive (i.e., the upper quartile) and negative (i.e., the lower quartile) TNI index values are in bold and italic, respectively.

Ranking	Year	ENSO phase in spring	TNI index (detrended)
52	1958	El Niño decays	-0.61 (-0.49)
53	1955	La Niña persists	-0.27 (-0.16)
54	2001	La Niña decays	0.21 (0.50)
55	1986	El Niño develops	-0.39 (-0.16)
56	1988	El Niño transitions to La Niña	-0.37 (-0.13)
57	1987	El Niño persists	0.10 (0.34)
58	1992	El Niño decays	0.21 (0.47)
59	1952	Neutral	-0.67 (-0.57)
60	1951	La Niña transitions to El Niño	-0.31 (-0.22)
61	1950	La Niña persists	0.77 (0.86)

Table S3. Prescribed SSTs in the tropical Pacific region for each model experiment. All model experiments are initiated from April of the prior year to December of the modeling year. For instance, in EXP_TNI, the model is integrated for 21 months starting in April using the composite April SSTs of 1956, 1964, 1973, 1998, and 2007.

Experiments	Prescribed SSTs in the tropical Pacific region
EXP_CLM	Climatological SSTs are prescribed in the tropical Pacific region (15°S–15°N; 120°E-coast of the Americas).
EXP_TNI	Composite SSTs of the five positive phase TNI years transiting from a La Niña identified among the ten most active U.S. tornado years (1957, 1965, 1974, 1999, and 2008) are prescribed in the tropical Pacific region.
EXP_LAN	Composite SSTs of the four years with a La Niña transitioning (1950, 1951, 1955 and 2001) identified among the ten least active U.S. tornado years are prescribed in the tropical Pacific region.
EXP_ELN	Composite SSTs of the four years with an El Niño transitioning (1958, 1987, 1988 and 1992) identified among the ten least active U.S. tornado years are prescribed in the tropical Pacific region
EXP_CPC	Same as EXP_TNI except that the composite SSTs are prescribed only in the western and central tropical Pacific region (15°S–15°N; 120°E - 110°W).
EXP_EPW	Same as EXP_TNI except that the composite SSTs are prescribed only in the eastern tropical Pacific region (15°S–15°N; 110°W-coast of the Americas).
EXP_011	SSTs for 2010-2011 are prescribed in the tropical Pacific region.
EXP_WPW	Same as EXP_011 except that the SSTs for 2010-2011 are prescribed only in the western Pacific region (15°S–15°N; 120°E - 180°).

SWD: Number of All U.S. Tornadoes (APR–MAY)

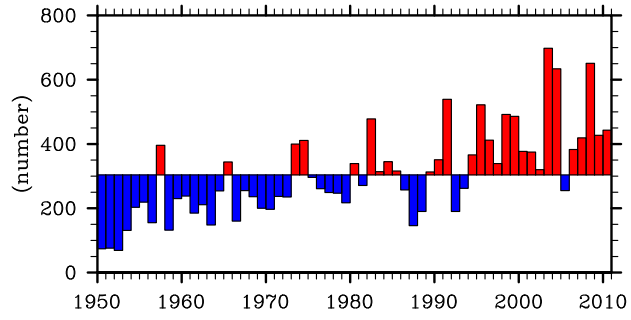


Figure S1. The number of all (F0 – F5) U.S. tornadoes for the most active tornado months of April and May (AM) during 1950-2010 obtained from SWD.

SWD: U.S. Tornadoes (APR–MAY)

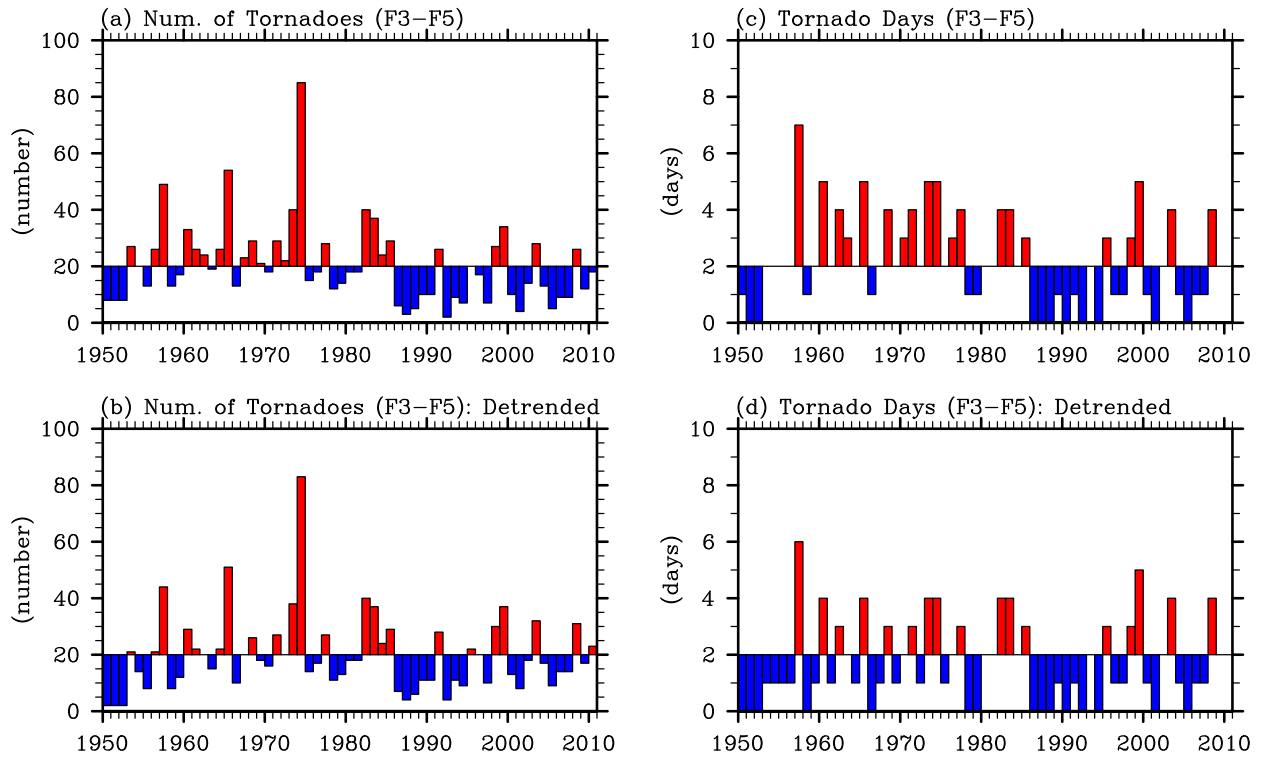


Figure S2. (a) The number of intense (F3 – F5) U.S. tornadoes and (c) the intense tornado-days for the most active tornado months of April and May (AM) during 1950-2010 obtained from SWD. The intense U.S. tornado-days is obtained by counting the number of days in which more than three intense tornadoes occurred. The detrended number of intense tornadoes and the detrended intense tornado-days are shown in (b) and (d), respectively.

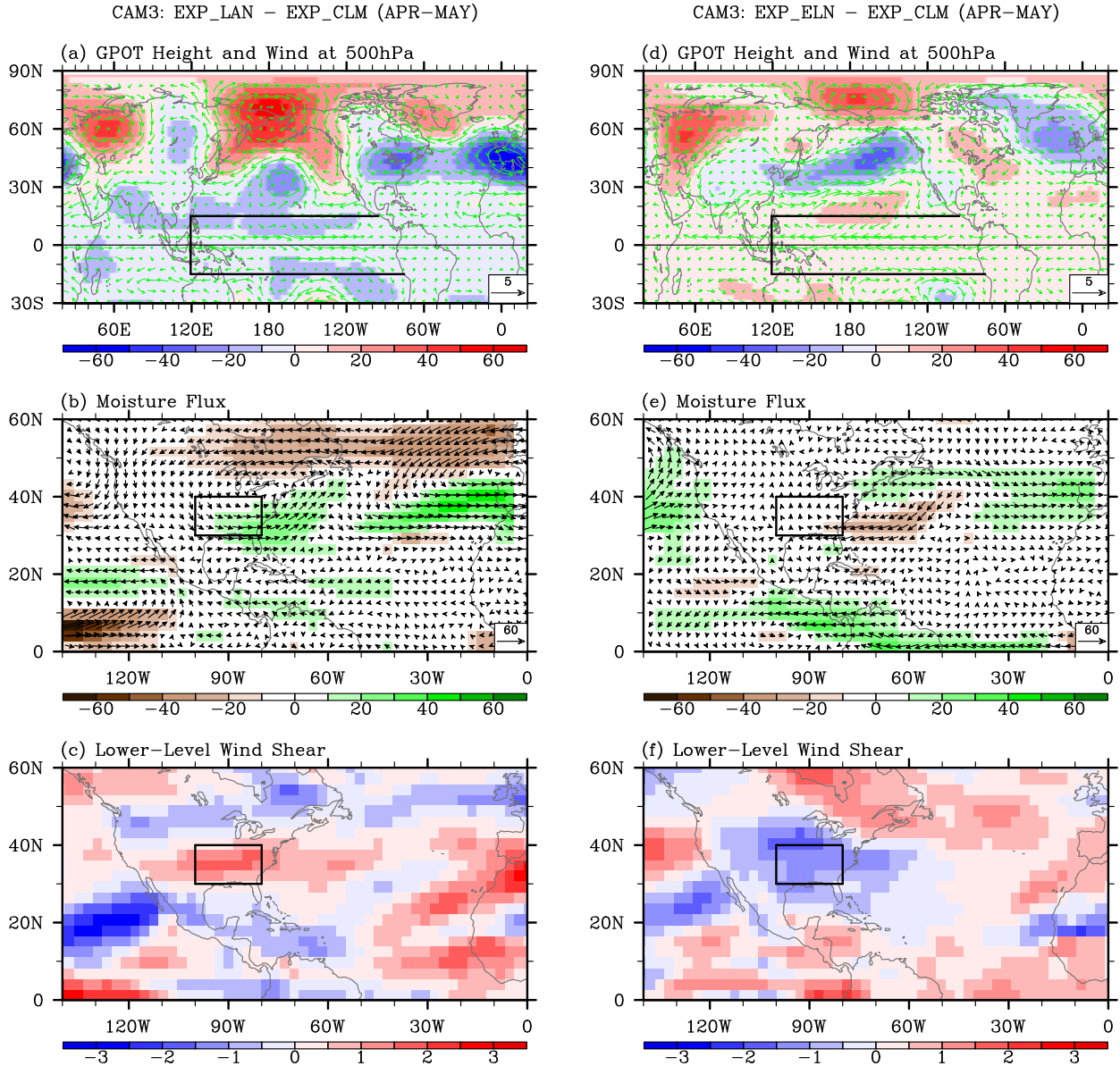


Figure S3. Simulated anomalous geopotential height and wind at 500, moisture transport and (c) lower-level (500 hPa – 925 hPa) vertical wind shear in AM obtained from EXP_LAN – EXP_CLM (a, b and c) and EXP_ELN – EXP_CLM (d, e and f). The unit is $\text{kg m}^{-1} \text{sec}^{-1}$ for moisture transport, m for geopotential height, and m s^{-1} for wind and wind shear. Thick black lines in (a) and (d) indicate the tropical Pacific region where the model SSTs are prescribed. The small box in (b), (c), (e) and (f) indicates the central and eastern U.S. region frequently affected by intense tornadoes.

CAM3: Convective Precipitation (APR-MAY)

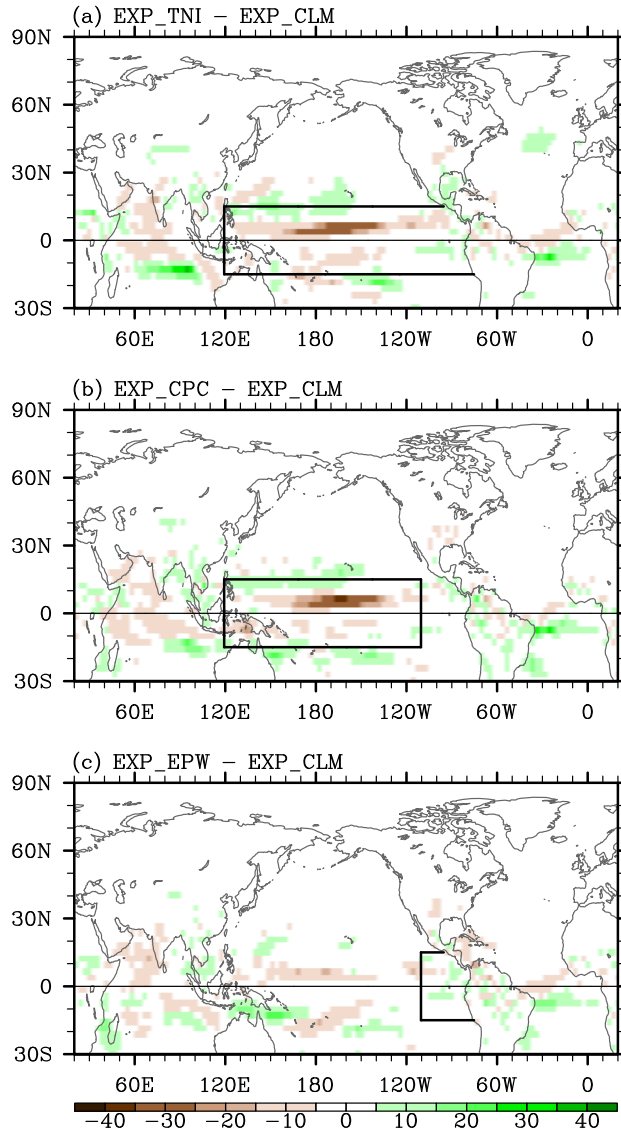


Figure S4. Simulated anomalous convective precipitation rate in AM obtained from (a) EXP_TNI - EXP_CLM, (b) EXP_CPC - EXP_CLM, and (c) EXP_EPW - EXP_CLM. The unit is mm day^{-1} . Thick black lines in (a) - (c) indicate the tropical Pacific region where the model SSTs are prescribed.

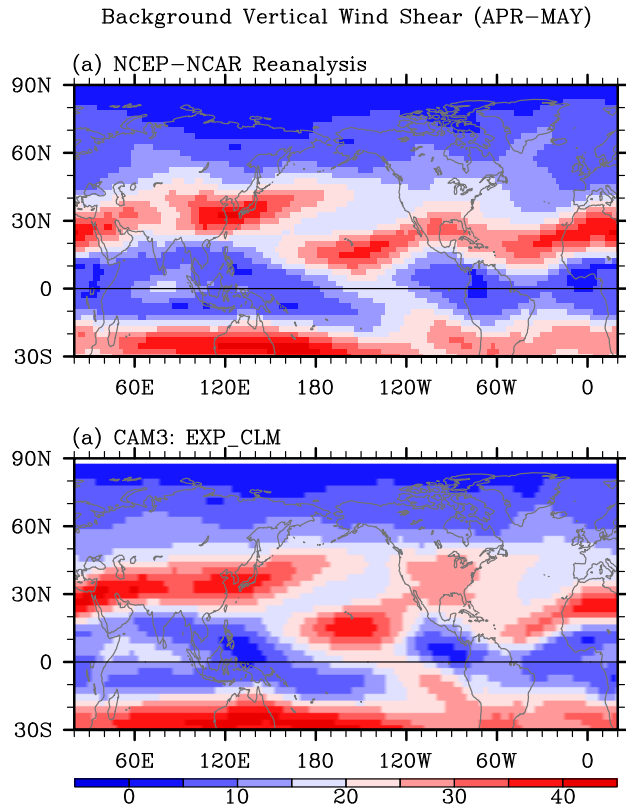


Figure S5. Background (climatological) vertical wind shear between 200 and 850 hPa in AM obtained from (a) NCEP-NCAR reanalysis, and (b) EXP_CLM. The unit is m sec^{-1} .

ERSST3: 2011 (APR-MAY)

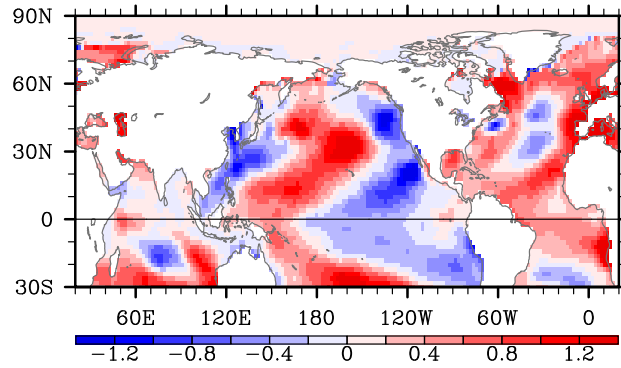


Figure S6. Anomalous SST in AM of 2011 obtained from ERSST3. The unit is °C.

NCEP-NCAR Reanalysis: 2011 (APR-MAY)

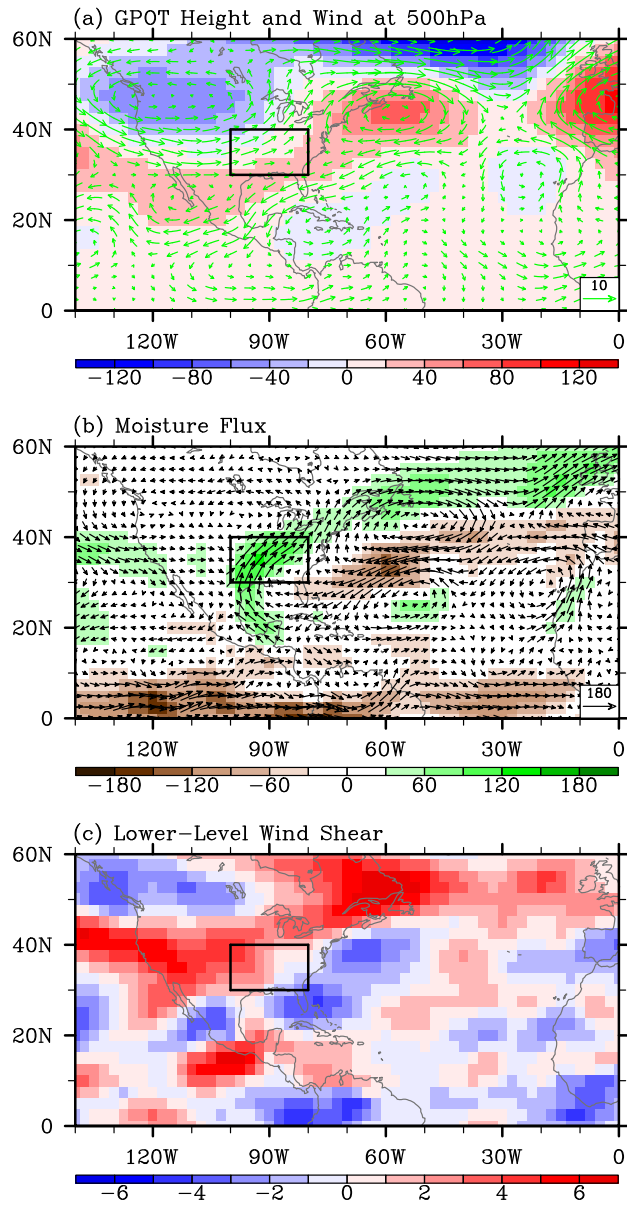


Figure S7. Anomalous (a) geopotential height and wind at 500 hPa, (b) moisture transport and lower-level (500 hPa – 925 hPa) vertical wind shear in AM of 2011. The moisture transport, geopotential height, wind and wind shear are obtained from NCEP-NCAR reanalysis. The unit is $\text{kg m}^{-1} \text{sec}^{-1}$ for moisture transport, m for geopotential height, and m s^{-1} for wind and wind shear. The small box in (a), (b) and (c) indicates the central and eastern U.S. region frequently affected by intense tornadoes.

CAM3: EXP_011 - EXP_CLM (APR-MAY)

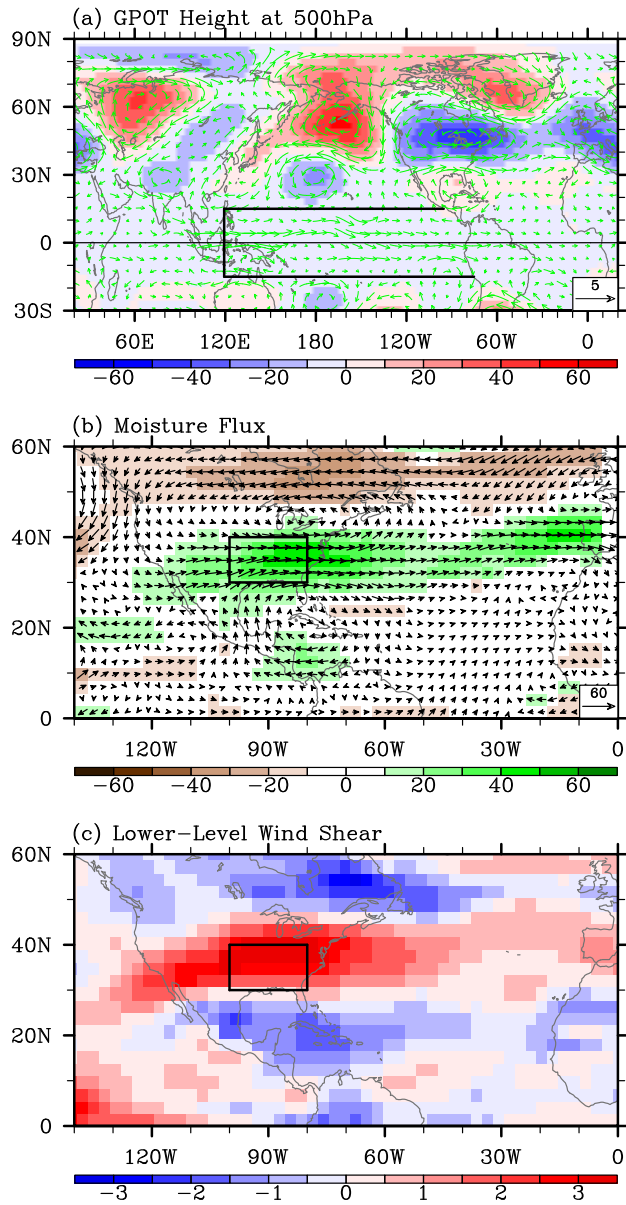


Figure S8. Simulated anomalous (a) geopotential height and wind at 500 hPa, (b) moisture transport and (c) lower-level (500 hPa – 925 hPa) vertical wind shear in AM obtained from EXP_011 – EXP_CLM. The unit is $\text{kg m}^{-1} \text{sec}^{-1}$ for moisture transport, m for geopotential height, m s^{-1} for wind and wind shear. Thick black lines in (a) indicate the tropical Pacific region where the model SSTs are prescribed. The small box in (b) and (c) indicates the central and eastern U.S. region frequently affected by intense tornadoes.

CAM3: EXP_WPW - EXP_CLM (APR-MAY)

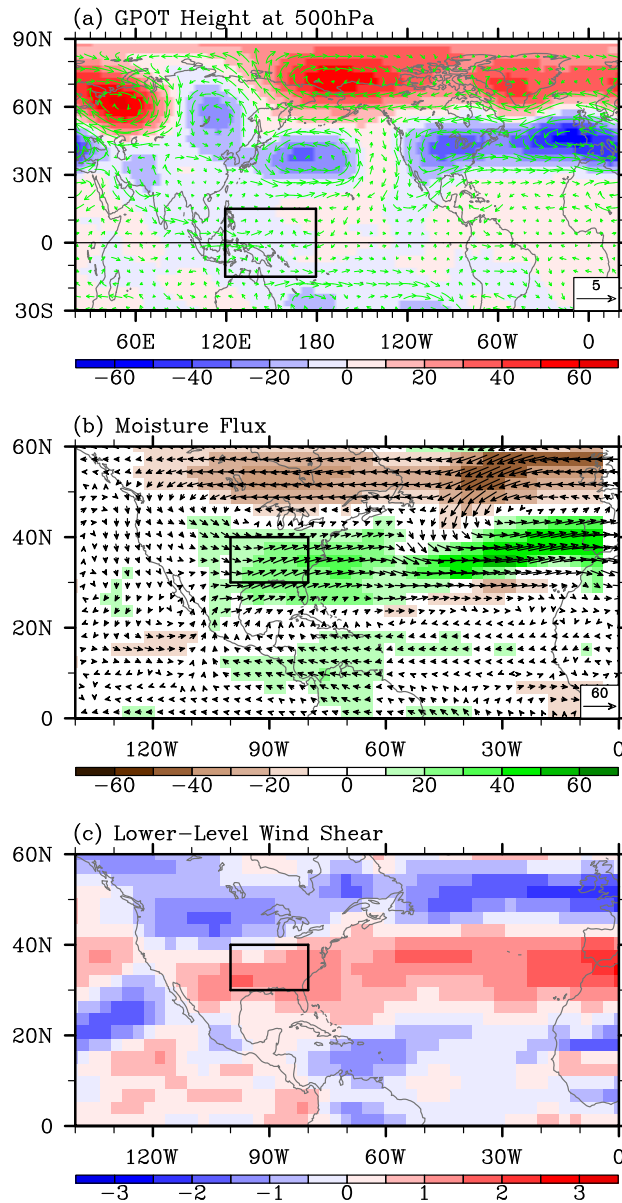


Figure S9. Simulated anomalous (a) geopotential height and wind at 500 hPa, (b) moisture transport and (c) lower-level (500 hPa – 925 hPa) vertical wind shear in AM obtained from EXP_WPW – EXP_CLM. The unit is $\text{kg m}^{-1} \text{sec}^{-1}$ for moisture transport, m for geopotential height, m s^{-1} for wind and wind shear. Thick black lines in (a) indicate the tropical Pacific region where the model SSTs are prescribed. The small box in (b) and (c) indicates the central and eastern U.S. region frequently affected by intense tornadoes.

CAM3: Convective Precipitation (APR–MAY)

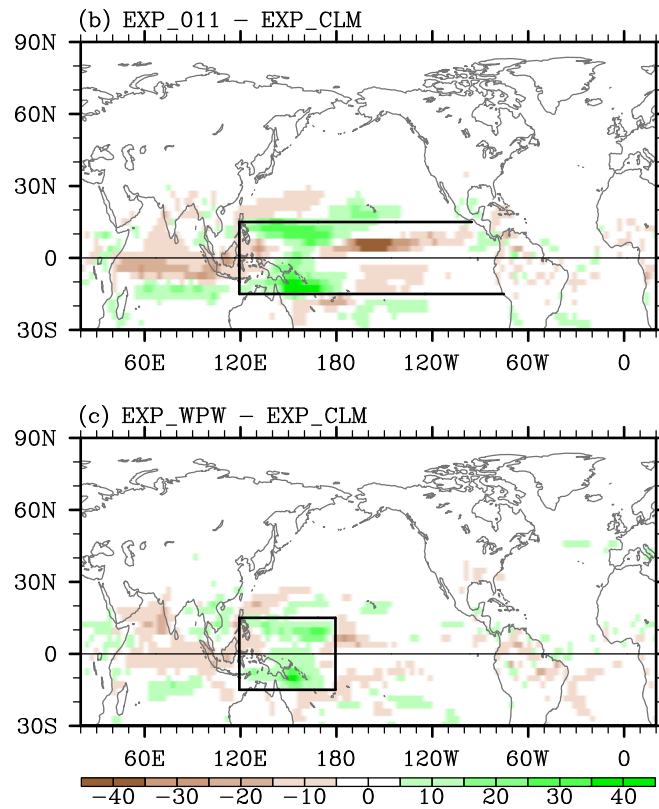


Figure S10. Simulated anomalous convective precipitation rate in AM obtained from (a) EXP_011 - EXP_CLM, and (b) EXP_WPW - EXP_CLM. The unit is mm day^{-1} . Thick black lines in (a) and (b) indicate the tropical Pacific region where the model SSTs are prescribed.